

YbPd₂In: a promising candidate to strong entropy accumulation at very low temperature

F. Gastaldo,¹ S. Gabani,² A. Džubinská,³ M. Reiffers,⁴ G. Pristáš,⁵ I. Čurlík,⁴
P. Skyba,² M. Clovecko,² F. Vavrek,² J. G. Sereni,⁶ and M. Giovannini⁷

¹*Department of Chemistry, University of Genova, Via Dodecaneso 31, Genova, Italy*

²*Institute of Experimental Physics, SAS, Košice, Slovakia*

³*Faculty of Natural Sciences, P.J. Šafárik University, Košice, Slovakia*

⁴*Faculty of Humanities and Natural Sciences, University of Prešov, 17. novembra 1, Prešov, Slovakia*

⁵*Institute of Experimental Physics, SAS, Kosice, Slovakia*

⁶*Low Temperature Division, CAB-CNEA, 8400 San Carlos de Bariloche, Argentina*

⁷*Department of Physics and CNR-SPIN, University of Genova, Via Dodecaneso 33, Genova, Italy*

We report on synthesis, crystal structure, magnetic, thermodynamic and transport properties of the new compound YbPd₂In, crystallizing as a Heusler structure type. A trivalent state of the rare earth was determined by fitting the magnetic susceptibility with a Curie-Weiss law. This compound is characterized by showing very weak magnetic interactions and a negligible Kondo effect. A specific heat jump was observed at $T \approx 250$ mK, followed at higher temperature by a power law decrease of $C_P(T)/T$. The resulting large electronic entropy increase at very low temperature is rapidly shifted to higher temperature by the application of magnetic field. This magnetocaloric effect places YbPd₂In as a very good candidate for adiabatic demagnetization cooling processes.

PACS numbers: 71.27.+a; 75.30.-m; 75.30.Mb

I. INTRODUCTION

Along decades, cerium and ytterbium intermetallics attracted continuous attention owing to the variety of anomalous physical phenomena discovered on their compounds^{1–4}. Recently notable examples of unique properties have been found in the Yb-T-X systems (T = transition metals, X = p-type elements). For instance, in a systematic search for new ytterbium-palladium indides and stannides^{5,6}, we have synthesized Yb₂Pd₂Sn, where two quantum critical points (QCPs) occur under pressure^{7,8} and under Sn/In doping⁹.

Prominent examples with platinum are given by the hexagonal YbPt₂Sn and the cubic Heusler YbPt₂In¹⁰. Interestingly, although crystal structures are different, these two compounds exhibit many common features, like stable trivalent Yb³⁺ magnetic moments in a framework of negligible Kondo effect and very weak exchange interactions. Moreover, both compounds are characterized by similar trends of C_m/T by temperature decreasing: an increase of C_m/T according of a power-law temperature dependence below 2 K, followed by broad anomalies at around 200 mK. It is worth noting that in these compounds C_m/T reaches record values up to 14 J/mol K². Similar features were found in YbCu_{5-x}Au_x ($0.4 < x < 0.7$), YbCo₂Zn₂₀ and YbBiPt, but showing a plateau in $C_m/T(T \rightarrow 0)$ at ≈ 7 J/mol K²^{11–13}, all implying high values of entropy increase at very low temperature.

The current interpretation for these unusual behaviors is that long range magnetic order is inhibited by very weak magnetic exchange or by magnetic frustration of Yb atoms placed in 2D (triangular) or 3D (tetrahedra) networks. Coincidentally, only very low Kondo effect affects their robust magnetic moments.

In some of these compounds, e.g. YbPt₂Sn and YbCo₂Zn₂₀, it was shown that the low temperature magnetic entropy is strongly shifted to higher temperature by applying magnetic fields, offering the interesting perspective to use these materials as efficient metallic refrigerant for adiabatic magnetization cooling^{8,14}.

In this work we report experimental results on crystal structure and physical properties of the new cubic Heusler indide YbPd₂In which, based on the present results of this paper, behaves similarly to the other members of the YbT₂X (T = Pt or Pd and X = Sn or In) family of compounds.

II. EXPERIMENTAL DETAILS

YbPd₂In polycrystalline samples, each with a total weight of 1.2 g, have been prepared by weighting the stoichiometric amount of elements with the following nominal purity: Yb 99.993 mass % (pieces, Yb/TREM purity, Smart Elements GmbH, Vienna, Austria), Pd 99.5 mass % (foil, Chimet, Arezzo, Italy), In 99.999 mass % (bar). In order to avoid the loss of ytterbium during the melting because of their high vapor pressure, the proper amounts of pure elements were enclosed in small tantalum crucibles sealed by arc welding under pure argon atmosphere. The samples were synthesized in an induction furnace under a stream of pure argon and annealed in a resistance furnace at 650 °C for three weeks. Finally the samples were quenched in cold water and characterized by optical and scanning electron microscopy (SEM) (EVO 40, Carl Zeiss, Cambridge, England), equipped with an electron probe microanalysis system based on energy dispersive X-ray spectroscopy (EPMA – EDXS). For the quantitative and qualitative analysis an accel-

eration voltage of 20 keV for 100 s was applied, and a cobalt standard was used for calibration. The X-ray intensities were corrected for ZAF effects. The annealed samples were crushed, powdered under pure acetone inside an agate mortar and studied by powder X-ray diffraction (XRD). The XRD data were collected at room temperature using the X'Pert MPD diffractometer (Philips, Almelo, The Netherlands) equipped with a graphite monochromator installed in the diffracted beam (Bragg Brentano, $\text{CuK}\alpha$ radiation). The theoretical powder pattern was calculated with the Powder-Cell program¹⁵. The FULLPROF program¹⁶ was used for Rietveld refinements. A Pseudo-Voigt profile shape function was used and full occupation with no atomic disorder was considered for all positions.

The thermodynamic and transport physical properties were performed by Physical Property Measurement System (PPMS) commercial device (Quantum Design) and PPMS Dynacool (Quantum design) in the 2 – 300 K temperature range with applied magnetic field up to 9 T. Specific heat was determined by means of the $2\text{-}\tau$ relaxation method. Electrical resistivity and magnetoresistance were measured using the 4-wire AC technique on the irregular samples shape in relative units. Magnetic properties were performed by Magnetic Property Measurement System (PPMS) (Quantum Design) in the temperature range of 2 – 300 K under applied magnetic fields up to 9 T. For temperature range below 1 K down to 80 mK, a ^3He - ^4He dilution cryogen-free refrigerator TRITON 200 (Oxford Instruments, UK) with 8 T magnet was used.

III. RESULTS

A. Crystal structure of YbPd_2In

In the course of a systematic investigation of the ternary Yb-Pd-In system a new ternary phase was found. A sample prepared on the stoichiometry 1:2:1 from SEM/EPMA revealed to be practically single phase. In fact, the XRD pattern of the compound (see Fig. 1) was successfully indexed by analogy with the corresponding known cubic phase YbPd_2Sn , which crystallizes with $cF16$ structure Cu_2MnAl -type (space group $Fm\bar{3}m$) with lattice parameters $a = 6.661(5)$ Å. Moreover, in agreement to SEM results, in XRD pattern no peaks belonging to spurious phases were found.

B. Magnetic properties

The temperature dependence of $1/\chi(T)$ inverse magnetic susceptibility for YbPd_2In is shown in Fig. 2. The measurements were done in the magnetic field of 1 T in the temperature range of 2–300 K. The susceptibility data can be accounted for with a modified Curie-Weiss

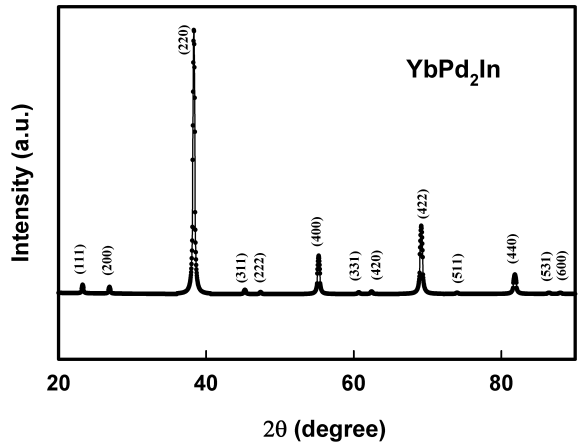


Figure 1. Powder x-ray diffraction pattern for YbPd_2In at room temperature. All reflexes were indexed according to the cubic Heusler phase structure type. Bragg peaks are indicated by the Miller indices.

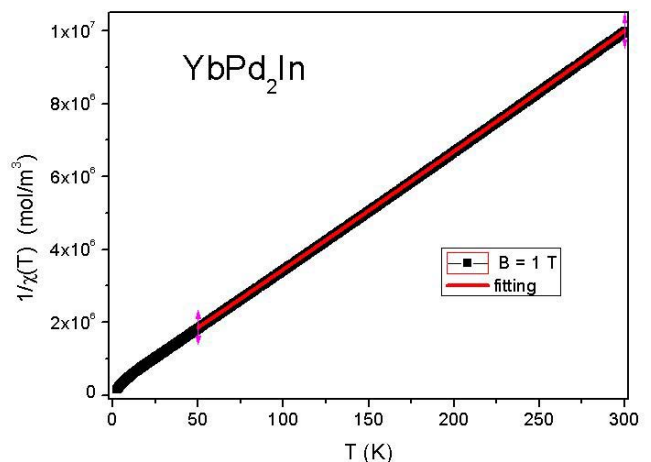


Figure 2. Temperature dependence of inverse susceptibility of YbPd_2In

(C-W) law given by the equation

$$\chi(T) = \chi_0 + \frac{c}{T - \Theta_P} \quad (1)$$

From the high temperature fitting of the dependence $1/\chi(T)$ the value of the effective moment for YbPd_2In is $\mu_{eff} = 4.49 \mu_B$ which is close to the free Yb^{3+} value ($\mu_{eff} = 4.54 \mu_B$). The paramagnetic Curie temperature obtained from the fit is $\Theta_P = -9$ K which is an indication of antiferromagnetic exchange interactions. Notably, no Pauli-like contribution χ_0 can be extracted from the fit in Fig. 2.

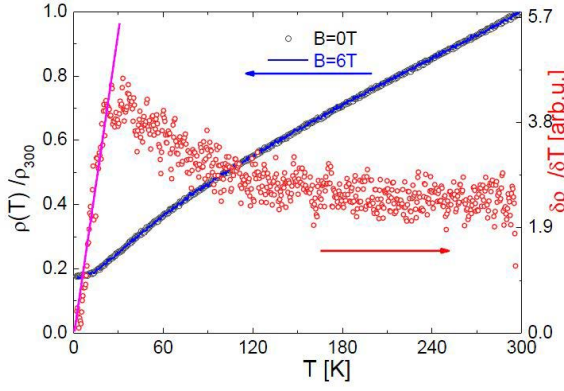


Figure 3. Left axis: temperature dependence of electrical resistivity of YbPd₂In normalized at room (300K) temperature. Right axis: electrical resistivity derivative showing a nearly linear increase between zero and about 25K.

C. Electrical resistivity

The normalized temperature dependence of electrical resistivity ($\rho(T)/\rho_{300K}$) of YbPd₂In, measured at magnetic fields of 0 T and 6 T, is shown in Fig. 3. The residual resistivity ratio $RRR \sim 5.5$ indicates a good quality of the polycrystalline sample, improving the $RRR \sim 2.2$ value of the YbPt₂Sn isotypic compound¹⁰ (the comparison with YbPt₂In is meaningless because this compound undergoes a CDW transition).

Focusing on the the positive curvature of $\rho(T)$ at low temperatures, the question arises about a coherent regime below 25 K. This feature is confirmed by the linear thermal variation of the $\delta\rho/\delta T$ derivative, which corresponds to the $\rho(T) = \rho_0 + AT^2$ dependence of a Fermi liquid (see the straight line in Fig. 3). On the other hand, the broad negative curvature centered around 70 K could be attributed to strongly hybridized CEF excited levels. However this scenario is not reflected in the straight line thermal dependence of $1/\chi$ shown in Fig. 2. Moreover, practically no magnetoresistance effect was detected. In fact, applied fields of $B = 3$ T (not shown) and 6 T produce no detectable effect on the the $\rho(T)$ dependence.

D. Specific heat of YbPd₂In

In Fig. 4 the specific heat $C_P(T)$ measurements performed at different magnetic fields (from 0 T to 9 T), within the $0.5 < T < 10$ K range, are shown. For $B = 0$ T a minimum in the heat capacity at around 4 K can be seen from which $C_P(T)$ increases continuously by temperature decreasing. This increase transforms into broad maximum centered at $T \approx 1.2$ K for $B = 1.5$ T under magnetic field, which shifts to higher temperature with increasing field intensity. These anomalies can be qualitatively described as Schottky-type anomalies which correspond to a two level system splitted by applied field.

Fig. 5 includes zero field $C_m(T)/T$ measurements per-

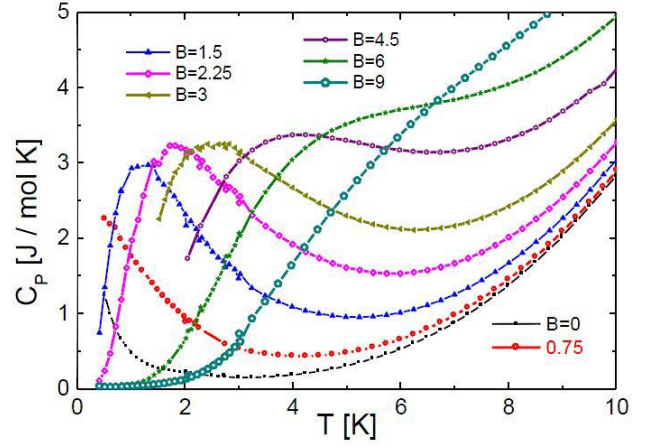


Figure 4. Thermal variation of the specific heat of YbPd₂In at zero and applied field up to $B=9$ T.

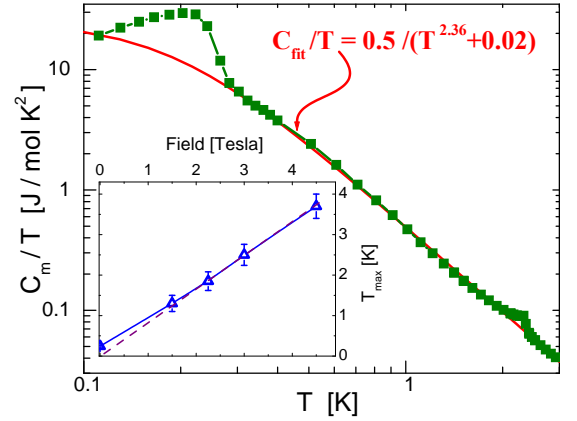


Figure 5. C_m/T vs T (at zero field) for YbPd₂In in a double logarithmic representation. The continuous curve C_{fit}/T represents a modified power law thermal dependence obtained within the $0.28 < T < 3$ K range. Inset: T_{max} with magnetic field, the dashed line represents a linear extrapolation to zero.

formed down to $T \approx 100$ mK in a $\log(C_m/T)$ versus $\log(T)$ representation up to $T = 3$ K. The magnetic contribution to specific heat C_m/T was obtained after subtracting a phonon contribution from the isotypic compound LuPt₂In compound¹⁷ with a low temperature phonon coefficient $\beta = 0.5$ mJ/mol K³. As it can be seen in the figure C_m/T decreases following a power law temperature dependence down to $T \approx 280$ mK where a jump in $C_m(T)$ occurs. At $T \approx 210$ mK C_m/T reaches the highest registered value for Yb-intermetallic compounds.

The small jump of $\Delta C_P = 53$ mJ/molK observed at $T = 2.2$ K is probably due to Yb oxide. It is worth noting that this effect is in coincidence with that reported for YbPd₂Sn¹⁸ and associated to a superconductive transition. Notably, this jump involves less than 1% of the electronic degrees of freedom and therefore it cannot be attributed to the Yb-4f electrons.

IV. DISCUSSION

The effect of magnetic field on the specific heat upturn below around 4 K reveals the formation of a Schottky-like anomaly (see Fig. ??) with the temperature of its maximum (T_{max}) increasing proportionally to the field intensity: $T_{max}/K \sim H/\text{Tesla}$ (see the inset in Fig. 5), whereas the value of the maximum (at $C_P \sim 3 \text{ J/mol K}$) barely increases. Above the anomaly $C_P(T > 6K, B)$ grows significantly with field, suggesting an increasing contribution of the excited CEF levels.

This Schottky-like anomaly in $C_P(T, B)$ indicates that the ground state (GS) of this compound can be described as a two level system with a splitting increasing proportionally to the field. Within the error in determining the exact temperature on the broad maxima, $T_{max}(B)$ extrapolates to $T_{max} = 0$ (see the dashed line in the inset of Fig. 5). However, since this compounds shows a transition around $T^* = 250 \text{ mK}$, it is evident that the weak interaction responsible for the transition is progressively overcome by the applied field (see the continuous curve in the inset of Fig. 5). The removal of the GS degeneracy by magnetic field produces a significant shift of the entropy to higher temperatures. This simple scenario may explain why YbT₂X compounds (T= Pd, Pt and X= In, Sn) are promising materials for adiabatic demagnetization in cooling processes.

As expected, $C_m(T)$ at zero field is not described by a Schottky-type anomaly. The analysis of the $C_m(T)/T$ dependence above the transition (i.e. between $0.3 \leq T \leq 3 \text{ K}$) shows that it can be properly fitted by a modified power law: $C_{fit}(T)/T = 0.5/(T^{2.3} + 0.02)$ as depicted in the double logarithmic representation of Fig. 5. This power law dependence strongly resembles that of the isotypic compounds YbPt₂X (X = In and Sn)¹⁰. In the case of these Pt homologues C_m/T increases with similar trend down to $\approx 0.20 \text{ K}$ where it practically flattens in YbPt₂In and slightly turns down in YbPt₂Sn.

Recent research has revealed a significant number of Yb-based intermetallic compounds showing (or even not showing) magnetic order down to around 300 mK, most of them exhibiting a power law dependence above that temperature^{10–13}. Two main reasons, which can act also simultaneously, can be argued for this scenario: magnetic frustration and extremely weak magnetic interactions. Some crystalline structures, such as fcc cubic structures, provide the proper configuration for geometric frustration¹⁹. The other inhibitor of long range magnetic order development is the presence of very weak inter-site magnetic interactions as proposed for the YbPt₂X homologues¹⁰. It is well known that in intermetallic compounds the dominant mechanism governing the magnetic exchange is the conduction electrons-mediated RKKY interaction:

$$T_{RKKY} \sim J_{ex} * \delta(E_F) * f(1/d^3) \quad (2)$$

where J_{ex} is the coupling parameter, $\delta(E_F)$ the density of the spin polarized band and $f(1/d^3)$ the envelopment of the decreasing-oscillating function. Although the quite large Yb-Yb spacing: $(d_{Yb-Yb}) = 4.7 \text{ \AA}$, may place YbPd₂In within the weakly magnetic interacting systems, magnetic order cannot be anyway excluded a priori for those interatomic spacings.

An empirical evaluation of the weight of the $\delta(E_F)$ factor can be extracted from the Sommerfeld coefficient: $\gamma \sim 6 \text{ mJ/mol K}^2$, of LuPd₂In reported by in Ref.¹⁷. This is a small value considering that the formula unit contains four atoms, whose respective individual γ values add up more than 30 mJ/mol K^2 . Thus, also the estimated $\delta(E_F)$ value for YbPt₂X compounds place YbPd₂In within the weak magnetic interacting systems.

The strength of the third factor: J_{ex} , can be evaluated from the low $|\theta_P|_{T \rightarrow 0}$. From a low temperature fitting of $1/\chi(T)$ we obtain for YbPd₂In a value of $|\theta_P|_{T \rightarrow 0} = -0.98 \text{ K}$. This number together with the lack of any Kondo interaction symptom also point to very weak J_{ex} intensity. Although the weakness of each one of these RKKY factors may guarantee the lack of magnetic order, their multiplicative character easily explains the small value of T_{RKKY} .

V. CONCLUSIONS

The newly synthesized cubic Heusler YbPd₂In compound was characterized in its structural, magnetic, thermodynamic and transport properties. At high temperatures the Yb atoms were found in their trivalent Yb³⁺ state. The absence of a significant Kondo effect is demonstrated by the very low value of θ_P and the continuous decrease of the electrical resistivity with temperature.

At low temperatures this compound shows its relevant properties with a very high $C_m/T \approx 30 \text{ J/molK}^2$ value at $T = 200 \text{ mK}$, reached after a power law increase of $C_m(T)/T$ that collects nearly 1/2 of the doublet GS entropy. Long range magnetic order is inhibited by a very weak exchange interaction down to $\approx 300 \text{ mK}$. Under magnetic field, the $C_m(T, B)$ behavior is properly described by a simple two level scheme which removes the GS degeneration by Zeeman splitting, whereas the weak magnetic interaction is quenched. The resulting associated entropy is rapidly shifted to higher temperature by the application of magnetic field, making YbPd₂In a promising candidate as metallic refrigerant for adiabatic demagnetization cooling.

VI. ACKNOWLEDGMENTS

This work was supported by the projects VEGA 2/0032/16 and European Microkelvin Platform APVV-17-0020.

-
- ¹ F. Steglich and S. Wirth, Rep. Progr. Phys. **79**, 084502 (2016).
 - ² P. Carretta, M. Giovannini, M. Horvatic, N. Papinutto, and A. Rigamonti, Phys. Rev. B **68**, 220404 (2003).
 - ³ L. S. Wu, W. J. Gannon, I. A. Zaliznyak, A. M. Tsvelik, M. Brockmann, J.-S. Caux, M. S. Kim, Y. Qiu, J. R. D. Copley, G. Ehlers, A. Podlesnyak, and M. C. Aronson, Science **352**, 1206 (2016).
 - ⁴ P. Carretta, R. Pasero, M. Giovannini, and C. Baines, Phys. Rev. B **79**, 020401 (2009).
 - ⁵ M. Giovannini, R. Pasero, and A. Saccone, Intermetallics **18**, 429 (2010).
 - ⁶ F. Gastaldo, M. Giovannini, A. Strydom, R. Djoumessi, I. Čurlík, M. Reiffers, P. Solokha, and A. Saccone, J. Alloy Compd. **694**, 185 (2017).
 - ⁷ T. Muramatsu, T. Kanemasa, T. Kagayama, K. Shimizu, Y. Aoki, H. Sato, M. Giovannini, P. Bonville, V. Zlatic, I. Aviani, R. Khasanov, C. Rusu, A. Amato, K. Mydeen, M. Nicklas, H. Michor, and E. Bauer, Phys. Rev. B **83**, 180404 (2011).
 - ⁸ H. Yamaoka, N. Tsujii, M.-T. Suzuki, Y. Yamamoto, I. Jarrige, H. Sato, J.-F. Lin, T. Mito, J. Mizuki, H. Sakurai, O. Sakai, N. Hiraoka, H. Ishii, K.-D. Tsuei, M. Giovannini, and E. Bauer, Sci. Rep. **7**, 5846 (2017).
 - ⁹ E. Bauer, G. Hilscher, H. Michor, C. Paul, Y. Aoki, H. Sato, D. Adroja, J.-G. Park, P. Bonville, C. Godart, J. Sereni, M. Giovannini, and A. Saccone, J. Phys.: Condens. Matter **17**, S999 (2005).
 - ¹⁰ T. Gruner, D. Jang, A. Steppke, M. Brando, F. Ritter, C. Krellner, and C. Geibel, Journal of Physics Condensed Matter **26**, 485002 (2014).
 - ¹¹ I. Čurlík, M. Giovannini, J. Sereni, M. Zapotokovǎ, S. Gabáni, and M. Reiffers, Phys. Rev. B **90**, 224409 (2014).
 - ¹² M. Giovannini, I. Čurlík, F. Gastaldo, M. Reiffers, and J. Sereni, J. Alloy Compd. **627**, 20 (2015).
 - ¹³ J. Sereni, J. Low Temp. Phys. (2017), 10.1007/s 10909-017-1828-5.
 - ¹⁴ Y. Tokiwa, B. Piening, H. S. Jeevan, S. L. Bud'ko, P. C. Canfield, and P. Gegenwart, SCIENCE ADVANCES **2**, e1600835 (2016).
 - ¹⁵ W. Kraus and G. Nolze, Journal of Applied Crystallography **29**, 301 (1996).
 - ¹⁶ J. Rodríguez-Carvajal, Physica B **192**, 55 (1993).
 - ¹⁷ D. Jang, T. Gruner, A. Steppke, K. Mitsumoto, C. Geibel, and M. Brando, Nature Communications **6**, 8680 (2015).
 - ¹⁸ H. A. Kierstead, B. D. Dunlap, S. K. Malik, A. M. Umarji, Shenoy, and G. K., Phys. Rev. B **32**, 135 (1985).
 - ¹⁹ A. Ramirez, Annu. Rev. Mater. Sci. **24**, 453 (1994).